



Supporting Information

for *Small*, DOI: 10.1002/smll.201906206

Glycyrrhizic-Acid-Based Carbon Dots with High Antiviral Activity by Multisite Inhibition Mechanisms

Ting Tong, Hongwei Hu, Junwei Zhou, Shuangfei Deng, Xiaotong Zhang, Wantao Tang, Liurong Fang, Shaobo Xiao, and Jiangong Liang**

Supporting Information

Glycyrrhizic Acid-based Carbon Dots with High Antiviral Activity by Multisite Inhibition Mechanisms

Ting Tong, Hongwei Hu, Junwei Zhou, Shuangfei Deng, Xiaotong Zhang, Wantao Tang, Liurong Fang, Shaobo Xiao and Jiangong Liang**

1. Experimental Section

1.1. Synthesis of Cit-CDs

Cit-CDs were synthesized as reported by Yang et al.^[1] with slight modification. Briefly, 1.05 g citric acid monohydrate (5 mmol) and 335 μ L ethylenediamine were dissolved into 10 mL deionized water and thoroughly mixed. Next, the mixture was transferred into a Teflon-lined autoclave and maintained at 180 °C for 5 h. After cooling to room temperature naturally, the mixture was centrifuged at 10,000 rpm for 10 min to remove large precipitate and collect the supernatant, which was then filtered through a 0.22 μ m filter to further remove small precipitate. Finally, the Cit-CDs were obtained by dialysis against deionized water for 8 h with a cut-off molecular weight 500 Da dialysis bag, the deionized water was changed every 2 h during dialysis. and then freeze-dried for further use.

Before the addition of CDs in the cell medium for the exposure experiments, the stock solutions containing CDs were filtered through a 0.22 μ m PVDS syringe filter (Roth, Karlsruhe, Germany) to avoid bacterial contamination.

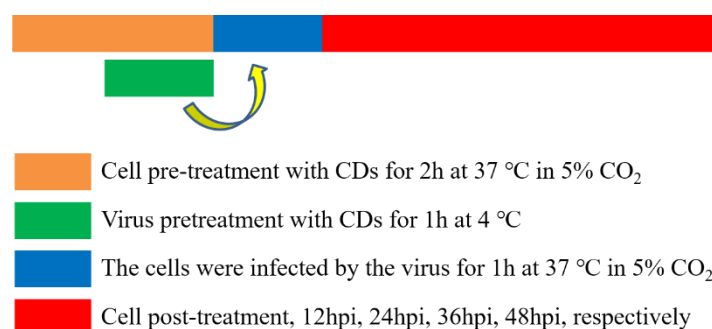
1.2. Characterization of CDs

All fluorescence measurements were carried out with an RF-5301PC fluorescence spectrometer (Shimadzu, Japan). The UV-vis absorption of all samples was measured on a UV-2450 spectrophotometer (Shimadzu, Japan). The Fourier transform infrared spectra (FT-IR) were recorded by a Nicolet Avatar-330 Fourier transform infrared spectrometer (Thermo Fisher Scientific, USA). The zeta-potential and size distributions were all measured with a dynamic light scattering (DLS) Malvern Zeta sizer instrument (Malvern ZEN 3690). The X-ray diffraction (XRD) was conducted with a D8 Advance X-ray Diffractometer (Germany), operated at 40 mA and 40 kV using Cu K α radiation with a wavelength of 0.2 nm. The scanning of the diffraction angle (2θ) was from 5° to 85° with a scanning speed of 10° /min. The surface morphology of the CDs was measured with a JEM-2100F, STEM/EDS high resolution transmission electron microscope (HR-TEM) (JEOL, Japan). The elemental and structural analysis of the CDs was performed using a ESCALAB Xi[†] photoelectron spectrum (XPS) instrument (Thermo Fisher Scientific, USA). ¹H NMR measurements were carried out for Cit-CDs using a Bruker Avance 600 MHz spectrometer (BRUKER, German), with Cit-CDs being dissolved in deuterated DMSO.

1.3. Antiviral Assay

The experimental process is shown in **Scheme S1**. Briefly, MARC-145 cells were incubated with CDs at 0.30 mg/mL in DMEM (containing 2% FBS) for 2 h. Meanwhile, RRRSV was preincubated with CDs at 0.30 mg/mL for 1 h at 4 °C. Then the medium containing CDs was removed and substituted with the pretreated PRRSV at multiplicity of infection (MOI) of 1. After incubation for 1 h, the supernatant was discarded, and cells were washed twice with DMEM, followed by incubation separately with CDs at 0.30 mg/mL for 12, 24, 36, and 48 h. The antiviral effect of Gly-CDs on PRRSV infection was then evaluated by plaque assay, IFA, western blot assay and RT-qPCR assay.

The antiviral effect of Gly-CDs on PEDV and PRV in Vero cells and PK-15 cells at the concentration of 0.30 mg/mL was detected in a similar way as described above.



Scheme S1. Antivirus experiment flow chart.

1.4. Plaque Assay

Briefly, MARC-145 cells were seeded into 6-well plates and cultured until ~100% confluence, followed by discarding the supernatant and adding the collected CDs samples to the cells by a 10-fold gradient dilution with DMEM (containing 2% FBS). After 1-2 h adsorption, the supernatant was removed and the cells were washed twice with DMEM to get rid of the non-absorbed virus particles. After adding to each well 2 ml of plaque fluid (48% 2 × DMEM, 48% low melting point agarose, 3% FBS, 1% kanamycin-streptomycin), the 6-well plate was placed at 4 °C for 15 min to coagulate the agarose, followed by incubation at 37 °C for 2-4 days. Then, the cells were stained at 37 °C for 1 h after adding to each well the 1:5 mixture of 1 ml of neutral red (3-Amino-7-dimethylamino-2-methylphenazine hydrochloride, Sigma) solution (2.0 mg/mL) and PBS. Finally, the supernatant was removed and the 6-well plate was stored overnight at 4 °C in the dark. The number of plaques was counted and virus titer was calculated.

1.5. Indirect Immunofluorescence Assay (IFA)

For binding assays, cells were seeded in a 24-well Ibidi μ -slide at low densities and cultured to 70-80% confluence at 37 °C and 5% CO₂. After treatment at the indicated time points, the MARC-145 cells on the μ -slides were washed three times with PBS, fixed with 400 μ l/well of 4% paraformaldehyde for 15 min at room temperature (RT) and permeabilized with 1 ml/well of precooled methanol for 10 min at RT. After three washes with PBS (5 min for each wash), the cells were blocked with 500 μ L/well of 5% (w/v) BSA at RT for 45 min or at 4 °C overnight. Then the cells were incubated with primary antibody for ~1 h. After washing three times with PBS, the cells were incubated with fluorescence-labeled secondary antibody in dark for 1 h. Subsequently, the cells were dyed with DAPI for 15 min in dark, followed by three washes with PBS. A confocal laser scanning microscope (Olympus IX73) was used to obtain the fluorescence images. The mouse mAbs against PRRSV nsp2 and N protein were prepared as described previously.^[2, 3] The mouse mAb against PEDV N protein was prepared by our laboratory.

1.6. Western Blot Assay

At indicated time points, MARC-145 cells were collected from 6-well plates. Next, cells were washed three times with precooled PBS, followed by treatment for 15 min with 150 μ L/well 2 \times lysis buffer A (LBA) (65 mM Tris-HCl with pH 6.8, 40% glycerin, 4% sodium dodecyl sulfate, 3% DL-dithiothreitol). After denaturing the cellular extracts by boiling water for 10 min in 5 \times sodium dodecyl sulfate (SDS, Beyotime, P0015L) loading buffer, equal amounts of samples were subjected to 12% sodium dodecyl sulfate polyacrylamide gel electrophoresis (SDS-PAGE). After separation by SDS-PAGE, the proteins were electroblotted onto 0.22 μ m PVDF membranes (Millipore, Billerica, MA) and blocked for 4 h with 10% (w/v) nonfat dry milk in Tris-buffered saline containing Tween 20 (TBST). After three washes with TBST (5 min per wash), the membranes were incubated with indicated

primary antibodies for 4 h and subsequently HRP-conjugated secondary antibodies for 1 h at 37 °C. Meanwhile, β -actin was detected as a loading control using mouse monoclonal antibody (mAb) against β -actin (Beyotime, AF0003). Protein bands were visualized using the Clarity Enhanced Chemiluminescence (ECL) reagent (Bio-Rad, Hercules, CA).

1.7. RNA Extraction

Total RNA was extracted from cells and viruses using RNA-Solv® Reagent (Omega Bio-tek). Briefly, 1 mL RNA-Solv® Reagent was directly pipetted into a 3.5 cm diameter culture dish to lyse the cells, followed by adding 0.2 mL chloroform per 1 mL RNA-Solv® Reagent and capping the sample tubes securely for 15 s vigorous vortexing. After incubation of the mixture on ice for 10 min and centrifugation at 12,000 rpm for 15 min, no more than 80% of the aqueous phase was transferred to a fresh microcentrifuge tube and mixed with 500 μ L isopropyl alcohol. After incubation for 10 min, the samples were centrifuged at 12,000 rpm for 10 min, followed by discarding the supernatant and mixing the pellet thoroughly with 1 mL 80% ethanol by vortexing. After centrifugation at 7,500 rpm for 5 min, the ethanol was aspirated and discarded, followed by air drying the RNA pellet for 2-5 min and supplementation of 50-75 μ L nuclease-free water or DEPC water (HyClone). The concentration of RNA was measured by a spectrophotometer (ND1000, Nanodrop Inc, Wilmington, Del).

1.8. Real-time Quantitative Reverse Transcription PCR (RT-qPCR) Assay

To evaluate the effect of Gly-CDs on PRRSV infection, the level of PRRSV ORF7 gene was detected. RNA (1 μ g) was reverse transcribed into cDNA using a Transcriptor First Strand cDNA Synthesis Kit (Roche) with oligo (dT) primers. The resulting cDNA was subsequently subjected to a SYBR green PCR assay (Applied Biosystems) incorporating

primers specific to PRRSV ORF7 gene (q5'UTR-F: GCATTTGTATTGTCAGGAGC, q5'UTR-R: AGCAGTGCAACTCCGGAAG). Each sample was assayed three times.

To explore the influence of Gly-CDs on PRRSV replication, the abundance of PRRSV negative-sense RNA transcript was tested with a similar method as described above. Briefly, the reverse transcription was conducted with primer (5'UF: GACGTATAGGTGTTGGCTC) binding to PRRSV negative-sense RNA, and the PCR assay was performed using primers specific to PRRSV 5'UTR (qORF7-F: GCAATTGTGTCTGTCGTC, qORF7-R: CTTATCCTCCCTGAATCTGAC).

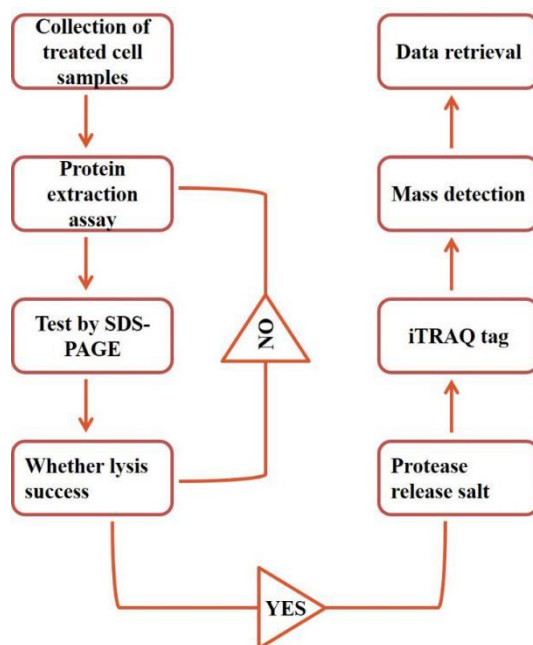
To detect the effect of Gly-CDs on the expression levels of ISGs, MARC-145 cells were incubated for 24 h with or without Gly-CDs at 0.30 mg/mL in DMEM (containing 2% FBS), then total RNA was extracted and reverse transcribed into cDNA with oligo (dT) primers. The primers specific to ISGs used in PCR assays are shown in **Table S1**.

Table S1: Primers used for RT-qPCR assay.

Primer	Primer sequence(5'to3')
GAPDH	TCATGACCACAGTCCATGCC
GAPDH	GGATGACCTTGCCCACAGCC
OAS-F	GATCTGACGCTGACCTGGTT
OAS-R	ACAGGCTTCCAGCTGTTTCC
ISG54-F	ACCTCTGGACTGGCAATAGC
ISG54-R	TGTCAGGATTCAGCCGAATG
ISG56-F	GGGTATGCGATCTCTGCCTAT
ISG56-R	TTAGACTGACAGCCTGCCTT
ISG60-F	GCTCCTTGCCAAACAGATGT
ISG60-R	TTTGGTGTGGATTCCAATGC
ZAP3-F	ACCCAGAGCTCCTTCTTCAC
ZAP3-R	CTGCTCGGATCTGGACTAGG

1.9. Preparation and Detection of Proteomic Samples

Isobaric tag for relative and absolute quantitation (iTRAQ) proteomic analysis was performed as shown in **Scheme S2**.



Scheme S2. iTRAQ proteomic analysis protocol used in this study.

1.9.1 Total protein extraction

Cell samples were taken from the $-80\text{ }^{\circ}\text{C}$ refrigerator, ground to powder at a low temperature, quickly transferred to a liquid nitrogen pre-cooled centrifuge tube, and supplemented with an appropriate amount of protein lysate (50 mM Tris-HCl, 8 M urea, 0.2% SDS, pH = 8). The mixture was shaken in an ice water bath for 5 min to allow proper lysis. After centrifugation at 12,000 g for 15 min at $4\text{ }^{\circ}\text{C}$, the supernatant was mixed with a final concentration of 2 mM DTTred and incubated for 1 h at $56\text{ }^{\circ}\text{C}$, followed by the addition of a sufficient amount of IAA to initiate the reaction at room temperature for 1 h in the dark. After adding 4-fold volume of $-20\text{ }^{\circ}\text{C}$ pre-cooled acetone to precipitate at $-20\text{ }^{\circ}\text{C}$ for at least 2 h, the mixture was centrifuged at $1\text{ }^{\circ}\text{C}$ for 15 min at $4\text{ }^{\circ}\text{C}$ to collect the precipitate. Then, the precipitate was resuspended in 1 mL $-20\text{ }^{\circ}\text{C}$ pre-cooled acetone and centrifuged at 12,000 g for

15 min at 4 °C. After discarding the supernatant, the precipitate was collected, and air-dried. Finally, the protein precipitate was dissolved by adding an appropriate amount of protein solution (8 M urea, 100 mM TEAB, pH = 8.5).

1.9.2. Protein examination

The BSA standard protein solution was prepared according to the manufacturer's instructions using a Bradford Protein Quantitation Kit with a concentration gradient of 50 to 1,000 µg/mL. The above BSA standard protein solutions and the samples of different dilution factors were added to the 96-well plate to make up the volume to 20 µL, and each gradient was repeated 3 times. Meanwhile, 200 µL of G250 staining solution was quickly added and allowed to stand at room temperature for 5 min to measure the absorbance at 595 nm. The standard curve method was used to calculate the protein concentrations of the samples. Each sample (30 µg protein) was subjected to 12% SDS-PAGE gel electrophoresis at 80 V for 20 min and 150 V for 60 min. After electrophoresis, Coomassie Brilliant Blue R-250 staining was performed, followed by washing in acetic acid until the protein bands were cleared.

1.9.3. iTRAQ mark

Briefly, 100 µg of protein sample was mixed with protein lysate to make up the volume to 100 µL, followed by supplementation of 2 µL of 1 µg/µL trypsin and 500 µL of 100 mM TEAB buffer and incubation at 37 °C overnight. Next, the solution was mixed with an equal volume of 1% formic acid and centrifuged at 12,000 g for 5 min at room temperature to collect the supernatant slowly through a C18 desalting column, followed by 3 washes in 1 mL of cleaning solution (0.1% formic acid, 4% acetonitrile). Then, 0.4 mL of eluate (0.1% formic acid, 45% acetonitrile) was added and the supernatant was eluted twice in succession. The eluted samples were combined and lyophilized. Reconstitution experiments were performed

by adding 20 μ L of 0.5 M TEAB buffer and enough iTRAQ labeling reagent (dissolved in isopropanol) to mix the samples by inverting for 1 h at room temperature. The reaction was stopped by adding 100 μ L of 50 mM Tris-HCl (pH = 8). After equal volume labeling, the samples were mixed, desalted and lyophilized.

1.9.4. Fraction separation

The mobile phase A solution (2% acetonitrile, 98% water, ammonia water adjusted to pH = 10) and phase B solution (98% acetonitrile, 2% water, and ammonia water adjusted to pH = 10) were prepared. The labeled sample powder was dissolved in 1 mL of A solution, centrifuged at 12,000 rpm for 10 min at room temperature, and a 1 mL volume supernatant was injected for HPLC fractionation using an L-3000 HPLC system on an XBridge Peptide BEH C18 column (25 cm \times 4.6 mm, 5 μ m). One tube was collected every minute, combined into 10 fractions, and lyophilized, with each being supplemented with 0.1% formic acid to dissolve.

1.10. Plasmid Construction and Transfection

Putative ATP-dependent RNA helicase DDX53 (DDX53) was amplified from the cDNA obtained from MARC-145 cells. Restriction enzyme sites were incorporated into the primer sequences to facilitate molecular cloning. PCR products were cloned into the pCAGGS-Flag vector to produce DDX53 expression vector. For transfection, cells were seeded in 6-well plates (Corning) and transfected at 70–80% confluency with respective constructed plasmids DNA by using Lipofectamine 3000 (Life Technologies), according to the manufacturer's instructions. After 24 h of transfection, the HP-PRRSV strain WUH3 was infected in MARC-145 cells at 36 h post transfection. Empty vector (Flag) transfection samples served as controls in the experiment.

1.11. Synthesized siRNA and Transfection

The target sequences were selected from the nitric oxide synthase (NOS3, Gene ID: 714231) using Ambion's web site tool to select potential siRNA. Then the siRNA was verified in inhibition effect by Western blot assay, and transfected into cells according to the manufacturer's instructions. Specifically, cells were seeded in 6-well or 24-well plates and transfected at 70-80% confluency with respective synthesized siRNA by RNA-mate (Genepharma, Shanghai, China), with the 24-well plate being transfected with 0.5 μg of siRNA per well while the 6-well plate being transfected with 4 μg of siRNA per well. After 24 h of transfection, PRRSV was inoculated, and at 36 hpi (hours of infection), samples were collected to examine the effect of siRNA on PRRSV proliferation. Negative control (NC) transfection samples served as controls in the experiment.

1.12. Purified PRRSV and Characterization by Electron Microscopy

PRRSV was purified as reported previously.^[4] Next, the purified virus was incubated with Gly-CDs or DMEM at 37 °C for 1 h. Phosphotungstic acid (PTA, pH = 7.0) was added for negative staining. Transmission electron microscopic images of PRRSV with or without Gly-CDs were obtained by an electron microscope (FEI Tecnai G² 20 TWIN).

2. Results

2.1. Characterization of Cit-CDs

The morphology and size distribution of the synthesized Cit-CDs were thoroughly investigated with transmission electron microscopy (TEM) and dynamic light scattering (DLS). The Cit-CDs were of a monodispersed, spherical round shape and uniform size, with a mean diameter of 6.0 nm calculated from the DLS size distribution (**Figure S1**). No apparent

lattice fringe could be observed, indicating that the Cit-CDs mainly consisted of amorphous carbon.^[5]

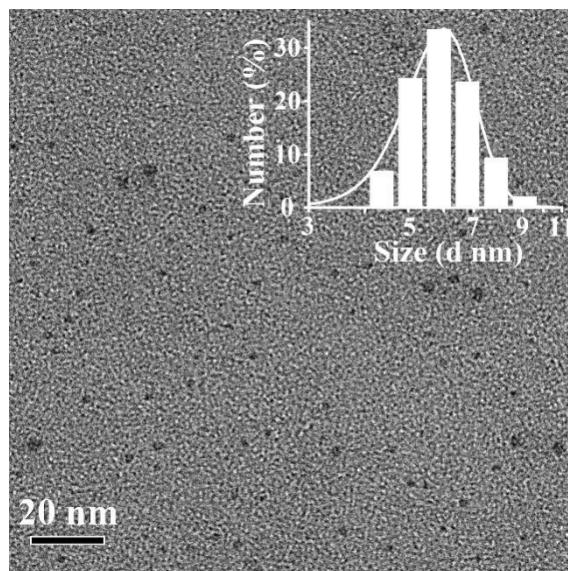


Figure S1. TEM image of Cit-CDs (Inset: DLS analysis of Cit-CDs).

Figure S2a shows the UV-vis absorption and FL spectra of the Cit-CDs. A characteristic absorption peak could be observed at 340 nm, corresponding to the $n-\pi^*$ transition of highly conjugated C=O and C=N bonds.^[6] The maximum emission of the Cit-CDs was centered at 455 nm whereas the maximum excitation was recorded at 349 nm. **Figure S2b** exhibits Cit-CDs emission spectra excited at a variety of excitation wavelengths, which presented an excitation independent emission. The result indicated that the fluorescence (FL) of the Cit-CDs was mainly generated from homogeneous emission.^[7]

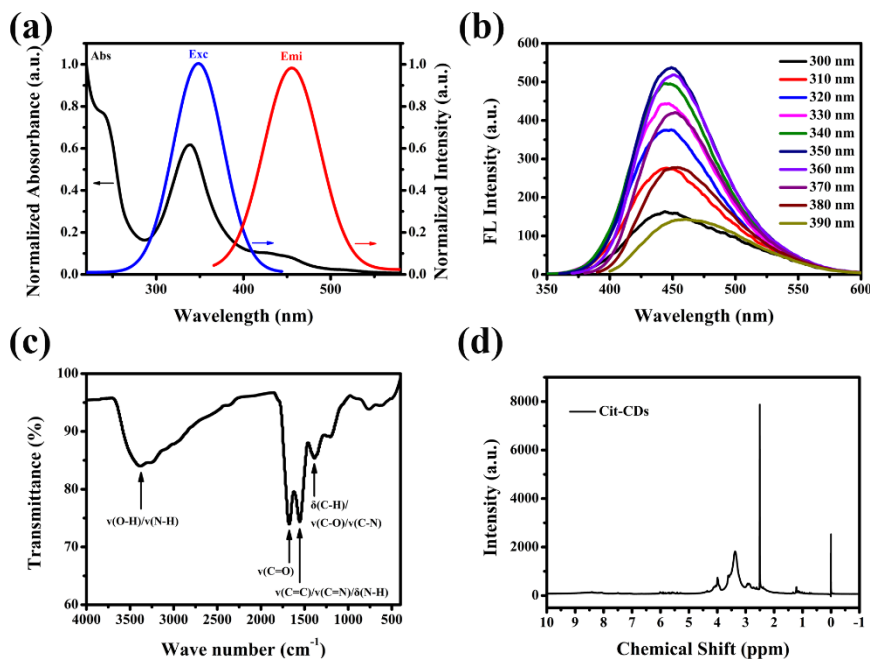


Figure S2. (a) UV-vis absorption (black), FL excitation (blue) and FL emission (red) spectra of Cit-CDs; (b) Cit-CDs FL emission spectra under the excitation of different wavelengths; (c) FT-IR spectrum of Cit-CDs and (d) ^1H NMR spectrum of Cit-CDs.

Figure S2d shows the ^1H NMR spectrum of the Cit-CDs. It can be seen that the chemical shifts of the hydrogen atoms in Cit-CDs were all below 10 ppm and mainly in the range of alkane and alkene domains, indicating the Cit-CDs are highly carbonized. The functional groups and elemental constituents of the Cit-CDs have been further characterized by Fourier transform infrared spectroscopy (FT-IR) and X-ray photoelectron spectroscopy (XPS). **Figure S2c** presents the FT-IR of the Cit-CDs. The absorption at 3380 cm^{-1} indicated the stretch vibration of O-H and N-H bonds, and the 1680 cm^{-1} peak was ascribed to the stretch vibration of C=O bonds. The absorption peaks at 1560 cm^{-1} and 1390 cm^{-1} showed the bending vibration of O-H and N-H bonds and stretch vibration of C=C, C=N and C-O on the aromatic rings.^[8, 9] The results of the FT-IR spectrum strongly suggested that the Cit-CDs were rich in -COOH and -NH₂ on the surface while the CDs possessed highly carbonized

polycyclic aromatic core.^[1] Figure S5a displays the full scan XPS spectrum of Cit-CDs, and elemental analysis indicated that the Cit-CDs consisted of 67.81% of carbon, 13.63% of nitrogen and 18.56% of oxygen. High-resolution XPS spectrum of C1s revealed the three fitting peaks of C=O, C-OH/C-O-C and C-C/C=C at 287.7 eV, 286.3 eV and 284.4 eV, respectively.^[1, 10] O1s high-resolution XPS spectrum of Cit-CDs could be resolved into two peaks at 531.8 eV and 530.4 eV, corresponding to C-N and N-H signals. The relatively higher intensity of N-H than C-N indicated the Cit-CDs are rich in amino groups on the surfaces.^[11] O1s could also be resolved into two peaks at 531.8 eV and 530.4 eV, indicating the C-OH/C-O-C and C=O signals in Cit-CDs.^[8]

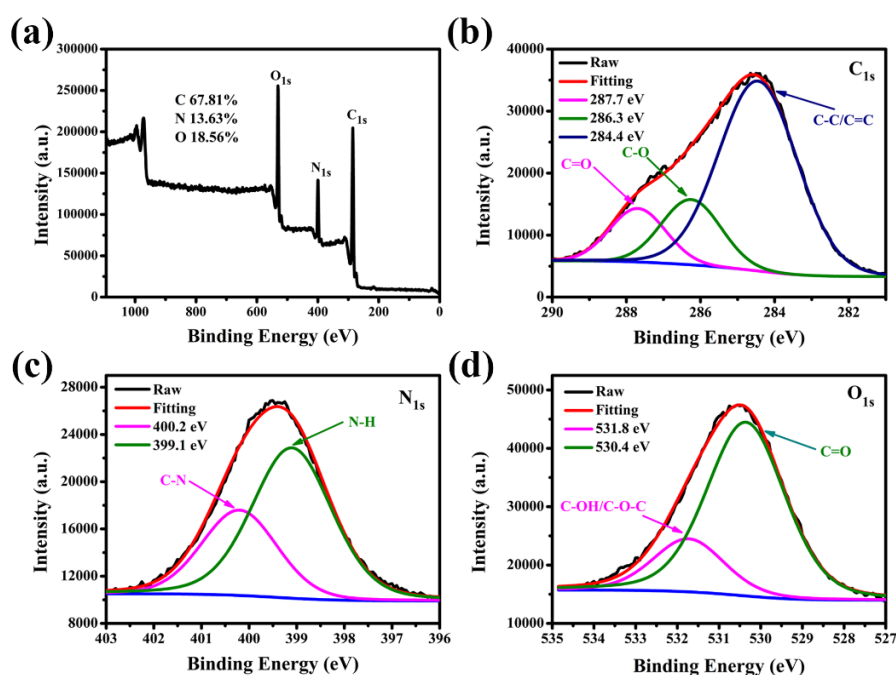


Figure S3. (a) Full scan XPS (inset percentage showed the relative content of each element in Cit-CDs) and high-resolution (b) C1s, (c) N1s and (d) O1s XPS spectra of the Cit-CDs.

2.2. Cytotoxicity of Gly-CDs, Cit-CDs and Glycyrrhizic Acid on MARC-145 Cells

To test the effect of the drug on the viability of MARC-145 cells, cytotoxicity assay was performed. The morphology of MARC-145 cells treated with the drugs for 36 hours is shown in **Figure S4**. We can clearly see that the cell growth remains completely normal after treatment of MARC-145 cells with a concentration of 0.90 mg/mL of CDs. However, after treating MARC-145 cells with glycyrrhizic acid at a concentration of 0.30 mg/mL, the morphology of the cells had some abnormalities. When the concentration reached 0.45mg/mL, the cells could not maintain their normal morphology, which fully demonstrates that the biocompatibility of glycyrrhizic acid is significantly improved after being transformed into CDs.

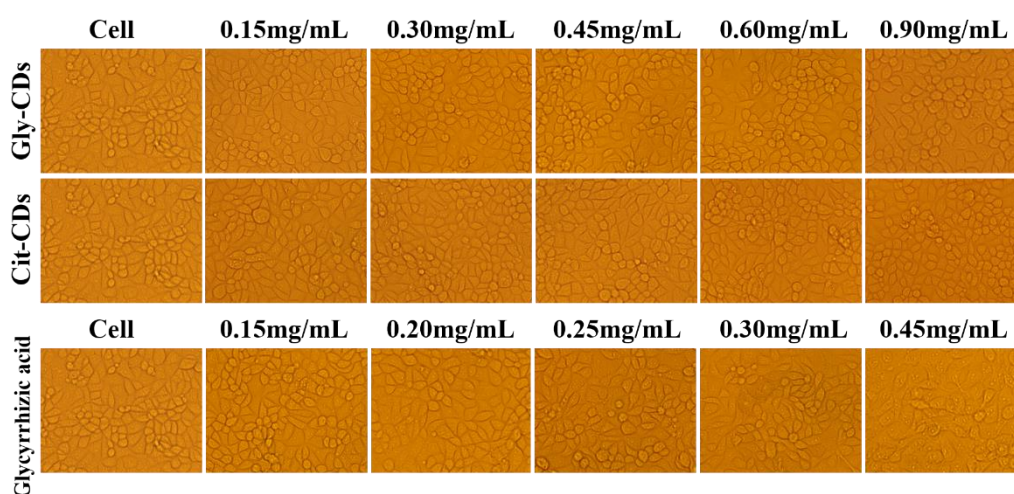


Figure S4. Cell morphology of MARC-145 cells treated with the drugs at different concentrations for 36 h.

Cytotoxicity assay results for Cit-CDs on MARC-145 cells is depicted **Figure S5**. It is clear that Cit-CDs are still not significantly cytotoxic at the indicated concentrations.

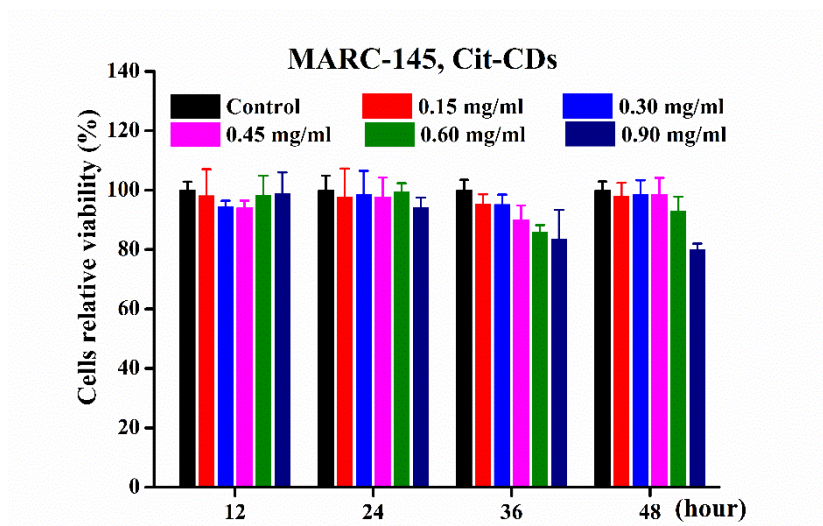


Figure S5. Cytotoxicity of Cit-CDs on MARC-145 cells. MARC-145 cells were incubated with Cit-CDs at the concentrations of 0, 0.15, 0.30, 0.45, 0.60 and 0.90 mg/mL for 12, 24, 36 and 48 h, respectively. Error bars represent the standard deviation from three repeated experiments.

2.3. Proteomic Sample Quality Testing

The collected cell samples were lysed, and the concentration, integrity, purity, and fragment size of the samples were examined by polyacrylamide gel electrophoresis. Our experimental results (**Figure S6**) fully meet the needs of subsequent experiments.

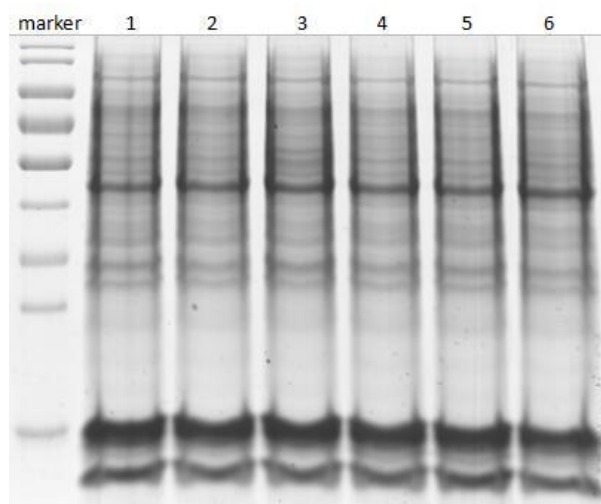


Figure S6. Protein sample quality inspection. 1, 2, 3, 4, 5 and 6 represent the mock group (parallel sample of 1 2 3) and the Gly-CDs treatment group (parallel sample of 4, 5, 6), respectively.

2.4. Differentially Expressed Proteins in Gly-CDs Treated MARC-145 Cells

Isotopically labeled relative and absolute quantitation (iTRAQ) is a relative and absolute quantification technique for in vitro isotope labeling developed by AB SCIEX. This technique utilizes multiple isotopic reagents to label the N-terminal or lysine side chain groups of a protein polypeptide. High-precision mass spectrometer serial analysis can simultaneously compare the protein expression between up to 8 samples. In recent years, high-throughput screening technology is commonly used in quantitative proteomics. In this study, a total of 60,036 peptides and 7,364 proteins were identified.

In order to improve the quality of the analysis results and reduce the false positive rate, the Proteome Discoverer 2.2 software was used to further filter the search results: Peptide Spectrum Matches (PSMs) with more than 95% confidence and proteins including at least one unique peptide (specific peptide) are considered as reliable. We only retained the reliable peptides and proteins by removing peptides and proteins with an FDR greater than 5%, then a total of 7,307 proteins were identified. In protein differential analysis, the pair of samples were first compared and then the ratio of the mean of all biological replicate quantitative values of each protein in the pair of comparative samples was compared as a fold change (FC). In order to judge the significance of the difference, the relative quantitative value of each protein in the two comparative samples was tested by T-test, and the corresponding p-value was calculated as a significant index. When $FC \geq 1.41$, and $p\text{-value} \leq 0.05$, the protein showed up-regulation. When $FC \leq 0.71$ and $p\text{-value} \leq 0.05$, the protein showed down-

regulation. A total of 7,307 proteins were identified, including 31 proteins that are differentially expressed (Total protein data and differentially expressed protein data can be found in the attached excel). A dot-plot was also provided here to give the overview of quantified proteins and differentially expressed cellular proteins (**Figure S7**). Red dots represent up-regulated proteins, green dots represent down-regulated proteins, and black dots represent non-differential proteins.

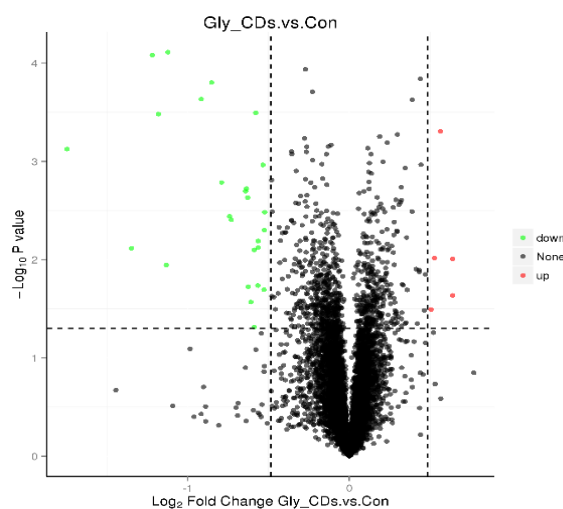


Figure S7. A dot-plot of the overview of quantified proteins and differentially expressed cellular proteins

2.5. Designing and Screening of Interference Molecules

We selected several down-regulated proteins that have been reported to be involved in viral proliferation as target proteins, and then designed corresponding interfering molecules based on these target proteins in order to investigate whether down-regulation of these proteins would affect the proliferation of PRRSV. As shown in **Figure S8**, we can select the best interfering molecules based on the results of the Western blot analysis.

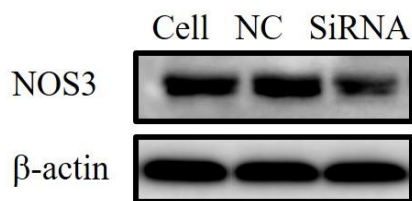


Figure S8. Verification of interfering molecules. The three bands in the figure represent the mock group, the negative control group, and the results of the expression of interfering molecules designed according to the target gene.

2.6. Effects of Down-regulation of Specific Proteins on the Proliferation of PRRSV

Down-regulated protein function analysis and reports have been mentioned in the main text. In order to verify the antiviral effect of knockout of NOS3, plaque assay was performed. As shown in **Figure S9**, the experimental results showed that they can all slightly inhibit the proliferation of PRRSV, and NOS3 exhibits the best inhibitory effect, with an inhibitory efficiency about 50%.

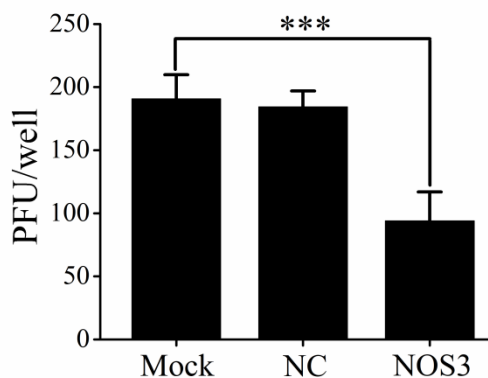


Figure S9. PRRSV proliferation under downregulation of NOS3 detected by plaque assay in MARC-145 cells. The mean value was calculated by the t test (mean \pm SD, n = 3). ***p < 0.001, compared with the indicated group.

2.7. Interaction between Gly-CDs and PRRSV

The interaction between Gly-CDs and the PRRSV particles was explored by incubating the purified PRRSV particles with Gly-CDs in vitro for 1 hour and the observed results are shown in **Figure S10**. In the TEM images, the single virus particle, single Gly-CDs, and Gly-CDs near the PRRSV particles are marked with red arrows.

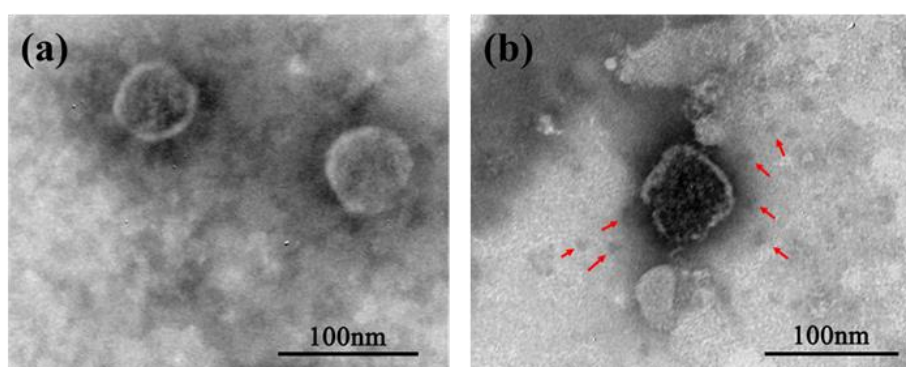


Figure S10. Transmission electron microscopic images of Gly-CDs bound on PRRSV particles. (a) PRRSV control, (b) PRRSV incubated with Gly-CDs for 1 h.

2.8. The Antiviral Activity of Gly-CDs with Different Hydrothermal Reaction Time

The hydrothermal reaction source, temperature and time have great effects on the size and functional groups of as-prepared CDs, which could further affect the antiviral activity of CDs.^[12] In our study, we compared the anti-PRRSV activity of Gly-CDs prepared under hydrothermal reaction for different time periods (7 h, 14 h) (**Figure S11**). The inhibitory effect of 14h-Gly-CDs was shown to be inferior to that of 7h-Gly-CDs, probably due to difference in functional groups of CDs.

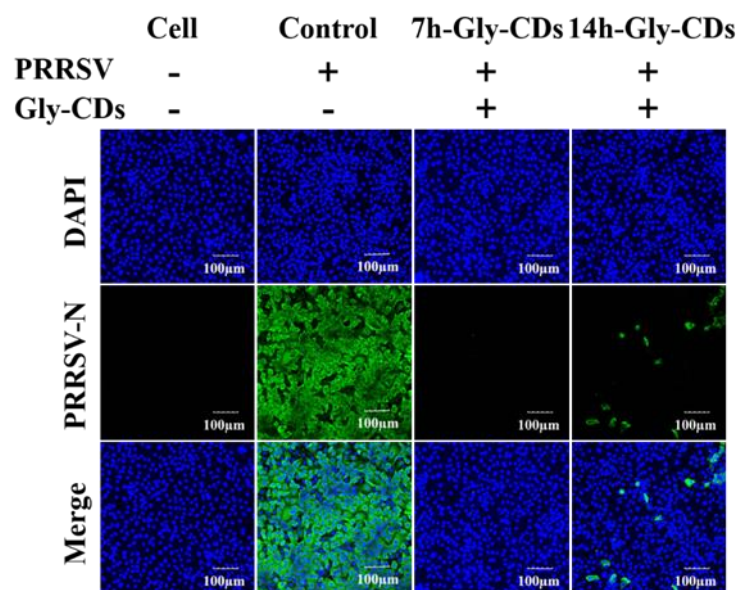


Figure S11. The antiviral activity of Gly-CDs at different hydrothermal reaction time periods. MARC-145 cells were mocked-infected or infected with PRRSV (MOI=1), and then untreated or treated with 0.30 mg/mL of Gly-CDs prepared under hydrothermal reaction for different time periods (7 h, 14 h). The immunofluorescence images of PRRSV-infected cells were taken at 48 hpi in the absence and presence of Gly-CDs. 7h-Gly-CDs and 14h-Gly-CDs refer to Gly-CDs which are prepared under hydrothermal reaction for 7 h and 14 h, respectively. The blue fluorescence signal stained with DAPI represents nuclei. The green fluorescence signal represents PRRSV N protein stained with mouse mAb specific for PRRSV N protein and Alexa Fluor 488-conjugated donkey anti-mouse IgG antibody.

References

- [1] S. Zhu, Q. Meng, L. Wang, J. Zhang, Y. Song, H. Jin, K. Zhang, H. Sun, H. Wang, B. Yang, *Angew. Chem. Int. Ed.* **2013**, *52*, 3953.
- [2] D. Wang, L. Cao, Z. Xu, L. Fang, Y. Zhong, Q. Chen, R. Luo, H. Chen, K. Li, S. Xiao, *PLoS One* **2013**, *8*, e55838.
- [3] T. Song, L. Fang, D. Wang, R. Zhang, S. Zeng, K. An, H. Chen, S. Xiao, *J. Proteomics* **2016**, *142*, 70.
- [4] S. Huang, J. Gu, J. Ye, B. Fang, S. Wan, C. Wang, U. Ashraf, Q. Li, X. Wang, L. Shao, Y. Song, X. Zheng, F. Cao, S. Cao, *J. Colloid Interface Sci.* **2019**, *542*, 198.
- [5] B. Zhi, M. J. Gallagher, B. P. Frank, T. Y. Lyons, T. A. Qiu, J. Da, A. C. Mensch, R. J. Hamers, Z. Rosenzweig, D. H. Fairbrother, C. L. Haynes, *Carbon* **2018**, *129*, 438.
- [6] R. Atchudan, T. Edison, K. R. Aseer, S. Perumal, N. Karthik, Y. R. Lee, *Biosens. Bioelectron.* **2018**, *99*, 303.
- [7] X. Miao, D. Qu, D. Yang, B. Nie, Y. Zhao, H. Fan, Z. Sun, *Adv. Mater.* **2018**, *30*, 1704740.
- [8] F. Zhang, X. Feng, Y. Zhang, L. Yan, Y. Yang, X. Liu, *Nanoscale* **2016**, *8*, 8618.
- [9] L. Deng, X. Wang, Y. Kuang, C. Wang, L. Luo, F. Wang, X. Sun, *Nano Res.* **2015**, *8*, 2810.
- [10] Y. Zhai, Z. Zhu, C. Zhu, J. Ren, E. Wang, S. Dong, *J. Mater. Chem. B* **2014**, *2*, 6995.
- [11] J. Schneider, C. J. Reckmeier, Y. Xiong, M. von Seckendorff, A. S. Sussha, P. Kasák, A. L. Rogach, *J. Phys. Chem. C* **2017**, *121*, 2014.
- [12] C. J. Lin, L. Chang, H. W. Chu, H. J. Lin, P. C. Chang, R. Y. L. Wang, B. Unnikrishnan, J. Y. Mao, S. Y. Chen, C. C. Huang, *Small* **2019**, *15*, e1902641.